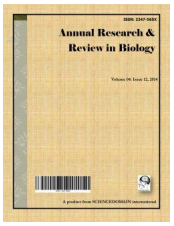

*Annual Research & Review in Biology*

*17(2): 1-17, 2017; Article no.ARRB.36163*
*ISSN: 2347-565X, NLM ID: 101632869*

# Nonglycine Residues in Proteins should most likely have an Allowed Conformation with a Negative Value for Backbone Torsion Angle $\phi$

**M. A. Basharov[1*]**

*[1]Institute of Theoretical and Experimental Biophysics, Russian Academy of Sciences, Pushchino, Moscow Region, 142290, Russia.*

***Author's contribution***

*The sole author designed, analyzed and interpreted and prepared the manuscript.*

***Article Information***

DOI: 10.9734/ARRB/2017/36163
Editor(s):
(1) George Perry, Dean and Professor of Biology, University of Texas at San Antonio, USA.
Reviewers:
(1) Nagendra Singh, Gautam Buddha University, India.
(2) Birsa Mihail Lucian, Alexandru Ioan Cuza University of Iasi, Romania.
(3) Ioana Stanciu, University of Bucharest, Romania.
(4) Rafael Trindade Maia, Universidade Federal de Campina Grande, Brazil.
(5) Emmanuel M. Papamichael, University of Ioannina, Greece.
Complete Peer review History: http://www.sciencedomain.org/review-history/20990

***Original Research Article***

***Received 16th August 2017***
***Accepted 1st September 2017***
***Published 14th September 2017***

## ABSTRACT

Backbone torsion angles $\phi$, $\psi$ of a vast majority of nonglycine residues in proteins lay within the peculiar insulated regions in the $(\phi,\psi)$ space assigned to the conformations allowed for nonglycine residues that embrace the conformations with negative and positive values of $\phi$ separately. Emphasizing this feature here, the abilities of nonglycine residues to access and reside in the allowed conformations with negative and positive value of angle $\phi$ evaluated from the alanine dipeptide $U(\phi,\psi)$ potential energy surface map computations. Established that for nonglycine residues the lowest energy conformation with negative value of $\phi$ is noticeably favorable than that with positive $\phi$ and these conformations are separated by unusually higher activation barrier. The occurrences of the residues in the conformations with negative and positive $\phi$ in a large set of high resolution structures from the Protein Data Bank also investigated. Taken together, the results suggested that nonglycine residues in proteins should most likely have an allowed conformation with negative value of angle $\phi$. Residues with positive $\phi$ angle are considered as outliers with a dubious conformation and should be inspected thoroughly for coordinate errors.

**Corresponding author: E-mail: m-basharov@rambler.ru;*

*Keywords: Amino acid; Dipeptide; conformational energy; protein; protein crystallography; protein structure; Ramachandran map; Ramachandran plot.*

## 1. INTRODUCTION

The knowledge of the accurate atomic coordinates, three-dimensional (3D) structure is essential for elucidating the function and interaction of proteins, definition of propensities of the individual common residues for secondary structure, dissection and assignment of secondary structure elements, for elaboration of effective predictive methods for the secondary and tertiary structures from the known amino acid sequence and validation tools based on the statistical techniques, and for comparative modeling of protein structures. The most powerful tool for determination of the 3D structure of proteins is X-ray crystallography. Qualitative high-resolution X-ray diffraction data from a protein crystal contain necessary information on the structure of the protein. Exploring the exact atomic coordinates from these data properly is not however an easy routine; introducing errors into the 3D structure model is almost unavoidable at almost all the stages of structure solution (determination of phases, interpretation of electron density map, fitting and building a trial structure model, rebuilding and refining the final model) [1-4]. As a result, serious errors will be present in a protein structure even carefully solved at an ultrahigh resolution [5-12].

Atomic coordinates define unambiguously the conformation of protein, characterized by a set of values of torsion angles $\phi$, $\psi$ and $\omega$ of the backbone and $_i$ of the side chain of consecutive residues of the polypeptide chain (Fig. 1a). In the approximation of all *trans*-peptide bonds, the backbone conformation can be described by angles $\phi$, and $\psi$ for the rotations about the *NC* and *CC* bonds. In a well-determined at a high or better (≤ 2 *Å*) resolution protein structure, the valence bonds and angles of the polypeptide are tightly adjusted to the accepted standard values and no objectionable nonbonded interatomic distances are present. The angles $(\phi,\psi)$ for a vast majority of nonglycine residues lay within the allowed regions of the alanine dipeptide classic $U(\phi,\psi)$ conformational, potential energy surface (PES) map [13-16], the Ramachandran map (Fig. 1b). Residues with the $(\phi,\psi)$ values from the disallowed region are specified as outliers, which is believed to be a result of errors upon structure solution or it may represent an unusual feature of the structure [14,17].

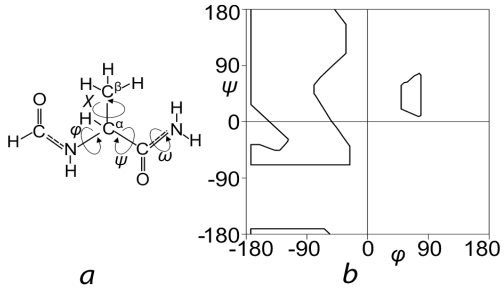


**Fig. 1. Schemes of alanine dipeptide and its classic *U* $(\phi,\psi)$ map**

*(a) The simplest alanine dipeptide, N-formyl-alanyl-amide (H–CONH–CH(CH₃)–CONH–H), with backbone atoms, valence bonds and torsion angles $\phi$, $\psi$ and $\omega$ labeled. (b) Alanine dipeptide classic U $(\phi,\psi)$ conformational energy map showing the allowed regions limited by closed solid curves defined using the lowest limits of the nonbonded interatomic distances (adapted from [15])*

Revision of the distribution of $(\phi,\psi)$ angles, the Ramachandran plot, has been an essential approach to assess the intrinsic quality and to judge the stereochemical and overall correctness of the protein model during a quarter of a century. The '$\phi,\psi$–criteria based' most popular tools PROCHECK [17-19], 'O' [10,20], and MolProbity [21-23] were devised and have been routinely used in protein structure improvements. Each tool specified the peculiar clearly demarcated regions of the conformations on the $(\phi,\psi)$ plane, the reference Ramachandran plot, allowed for nonglycine residues in proteins determined from the assiduous statistical analysis of a large set of high–resolution protein structures from the Protein Data Bank (PDB) [24,25]. PROCHECK discerned three types of the allowed regions (Fig. 2a), 'O' specified a single type of the allowed regions (Fig. 2b), MolProbity distinguishes Pro, pre–Pro and the rest general case of nonglycine residues and assigned to each category two types of the allowed regions (Fig. 2c).

Deviation of the Ramachandran plot of a protein from the reference Ramachandran plot can be used to assess the stereochemical quality of this structure and identify local main-chain inaccuracies. In this manner, nonglycine residues from the outside of the reference plot are considered as outliers with a dubious conformation. Nevertheless, the fact "However, these statistical techniques use a database of

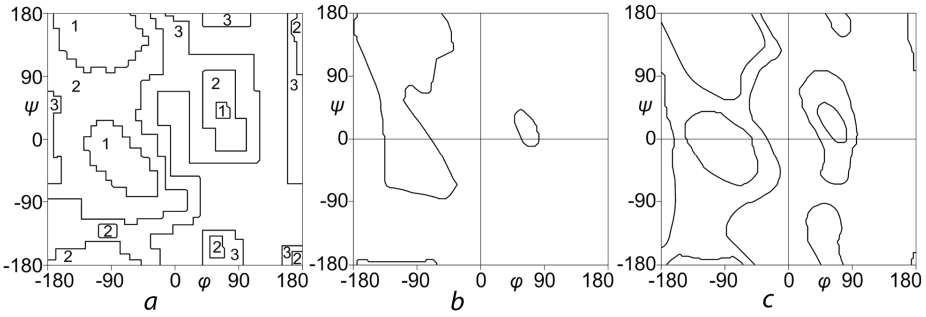


**Fig. 2. Allowed regions of *(ϕ,ψ)* chart for nonglycine residues suggested by the popular protein structure quality assessment tools limited by closed solid curves**

*(a) Allowed regions by ProCheck labeled: 1, most favored; 2, additionally allowed; 3, generously allowed (adapted from [18]). (b) Allowed regions by 'O' (adapted from [20]). (c) Allowed regions by MolProbity: 1, favored; 2, allowed (for non Pro or pre-Pro residues; adapted from [23])*

known structures, and the quality of the distributions is dependent on the quality of these known structures" [19] is well known. A more exact reference Ramachandran plot, defined from a duly objective statistical analysis of the richest database of best quality protein structures from the PDB, is believed to be required for further improvements of protein structure models [10,17-21], and such studies have been in progress [21-23,26-30].

A pronounced common feature of the area for allowed conformations for nonglycine residues of both classic Ramachandran map and the reference Ramachandran plots is plainly visible from Figs. 1b and 2 that it consists of the entirely insulated regions embracing the conformations with negative and positive values of torsion angle $\phi$ separately. With account of this feature in this study, the probability of nonglycine residues both to get and reside in, *i.e.* the rate and the equilibrium constants of the allowed conformations with negative and positive values of angle $\phi$ are estimated from the computation of alanine dipeptide *(ϕ,ψ)* conformational energy, *U(ϕ,ψ)* PES map. Inasmuch as alanine dipeptide is believed to represent conformational attributes of nonglycine and nonproline residues in a polypeptide chain quite satisfactorily; the main task is to assess the potential energy reasonably [13-16,31,32]. Occurrences of nonglycine residues in conformations with negative and positive values of $\phi$ in a large set of ≤ 2 *Å* resolution protein structures from the PDB are also analyzed. It is proposed that nonglycine residues in a native protein spatial structure should most likely have an allowed conformation with a negative value of backbone torsion angle $\phi$. Residues with positive $\phi$ are suggested as outliers with a dubious conformation and should be reviewed thoroughly for the reliability of the backbone atomic coordinates.

## 2. MATERIALS AND METHODS

### 2.1 Estimation of the Conformational Energy

Alanine dipeptide was modeled as N-formyl-alanyl-amide (Fig. 1a) using the standard bond lengths and angles given in [33]. The *U(ϕ,ψ)* PES map was computed at 10 intervals over the $\phi$ and $\psi$ torsion angles from –180 to 180. The potential energy was estimated by using the semi-empirical Bond-Bond Interactions (BBI) method [34,35]. The method is reliable enough, as it quite satisfactorily reproduces the available experimental or *ab initio* quantum-chemical data on the conformations, internal rotational barriers, and dipole moments of a wide range of organic molecules, the preferred structure, stable configurations, interaction energies, and dipole moments of dimers and complexes of such molecules. The method reproduces quite well also the *U(ϕ,ψ)* maps of dipeptides obtained by the *ab initio* quantum-mechanical methods available in the literature. More results of the related computations and additional references to the BBI method can be found in [35,36].

### 2.2 Database, Dataset and Data Analysis

From the PDB [24,25], the data on a set of protein structure models including the 195 high ≤ 2.0 *Å* resolution 'old', deposited in the PDB by 1992 structures and 130 ultrahigh ≤ 1.0 *Å* resolution largely nonhomologous protein structures deposited in the PDB by 2012 were selected arbitrary for the analyses. The backbone and side-chains bond lengths and

bond and torsion angles of amino acid residues in the selected structures were calculated from atomic coordinates. The conformity of nonbonded interatomic distances to the accepted lowest limits given in [14] and bond lengths and angles to the standard values given in [33] were verified.

For 195 high resolution 'old' structures, the identity and homology between the proteins were clarified. The signs of backbone torsion angle $\phi$ of the same and equivalent residues in the different structure models of the same and homologous proteins were compared. Based on the results, the highest resolution 52 largely non-homologous protein structures were picked out. These and the selected 130 ultrahigh-resolution structures were used in the final analysis. In this set of 182 structures, for the oligomeric proteins with identical subunits the data on one subunit were involved. It was the first subunit if the same or no nonglycine residues were with positive value of $\phi$ angle in the subunits and otherwise (a few cases) the subunit with the least number of nonglycine residues with positive value of $\phi$. The Ramachandran plots of nonglycine residues in every structure and of the total and individual common nonglycine residues in all structures were analyzed with rapt attention on the residues with positive value of torsion angle $\phi$. Every with positive $\phi$ nonglycine residue detected was inspected also in the other ≤ 2.0 *Å* resolution structure models of the corresponding protein in the 2014 release of the PDB if such was available, to ascertain whether or not this residue is with negative $\phi$ there. Thus more than four thousand protein structure models were analyzed.

Computations, data processing and data analyses were performed using personal programs in FORTRAN. The $U(\phi,\psi)$ PES map, $U(\phi)$ curve and $(\phi,\psi)$ distribution were plotted by SigmaPlot. Rest drawings were designed by CorelDRAW and Adobe Photoshop.

## 3. RESULTS AND DISCUSSION

### 3.1 The Conformational Energy Estimation Evinces: Backbone Torsion Angle $\phi$ of Nonglycine Residues in Protein Spatial Structure should have a Negative Value

Fig. 3 shows the alanine dipeptide $U(\phi,\psi)$ PES map obtained in the computations. In this study, the conformations of the dipeptide are assigned with the energy 10 *kcal/mol* or less as allowed, 20 *kcal/mol* or less as permissible and above 20 *kcal/mol* as disallowed. The definitions seem reasonable enough from several points of view including the following formals. The regions of the conformations specified as allowed (Fig. 3b), the allowed regions, resemble in appearance the known allowed regions reviewed above (Figs. 1b and 2) and especially that defined by the MolProbity. In the area of the conformations defined as permissible (Fig. 3a) which fits into the habitually disallowed region, the transition state saddle points and the kinetic pathways for the conformational transitions between the allowed regions can be distinguished.

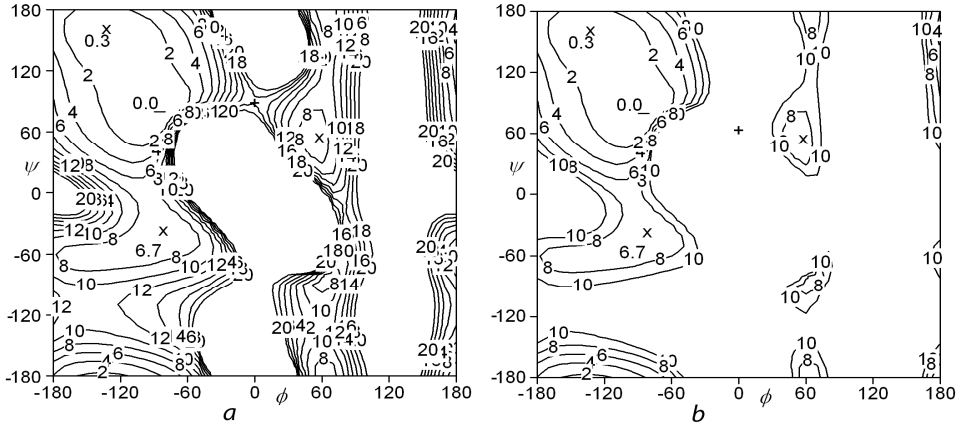


**Fig. 3. Alanine dipeptide $U(\phi,\psi)$ conformational energy map by the BBI method at 10 intervals**

*The equipotential energy contours are drawn at 2 kcal/mol intervals. The zero, lowest potential energy is designated by a circle, crosses show the local minima and pluses mark the saddle points. (a) $U(\phi,\psi)$ map with the potential energy contoured 20 kcal/mol and less showing the permissible region. (b) $U(\phi,\psi)$ map displaying the allowed regions, with the potential energy contoured 10 kcal/mol and less*

As seen from Fig. 3, the transitions between the regions of the allowed conformations with negative and positive values of $\phi$ is possible over the axis $\phi$ = 0°, over the saddle point nearly (0°, 90°), whereas such a transition is virtually impeded from any other side by an energy barrier exceeding 20 *kcal/mol*. Fig. 4 displays the preferable kinetic path for possible transitions. The path represents the profile of the lowest potential energy depending on torsion angle $\phi$ on the $U(\phi,\psi)$ map, the $U(\phi)$ profile plainly. On the $U(\phi,\psi)$ map, the values of potential energy at the conformations of the lowest energy in the allowed region with negative values of $\phi$ (~–80°, ~80°), local minimum in the allowed region with positive values of $\phi$ (~60°, ~50°) and saddle point between the allowed regions (~0°, ~90°) are of current interest. They determine the probabilities of both to acquire and reside, *i.e.* the rate and equilibrium constants of the allowed conformations with negative and positive values of angle $\phi$ for alanine residue. The values are estimated as 0 *kcal/mol* for the lowest-energy conformation with negative ($\phi$~ –80), 7.5 *kcal/mol* for the local minimum with positive ($\phi$~ 60) and 17.6 *kcal/mol* for the transition state ($\phi$~ 0°) (Fig. 4).

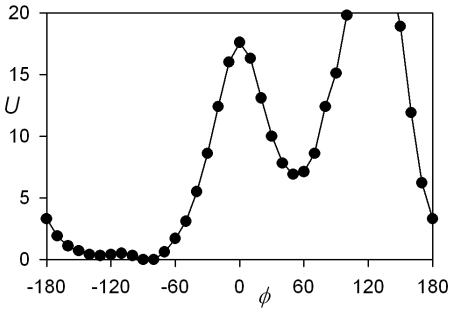


**Fig. 4. $U(\phi)$ profile of the lowest energy depending on torsion angle $\phi$, for alanine dipeptide**

*The value $U(\phi_i)$ (kcal/mol) for the given angle $\phi_i$ represents the minimum of the energy in the interval $0° \le \psi \le 180°$ on the $U(\phi,\psi)$ map (Fig. 3a) at fixed $\phi_i$*

Previously [36], the average values of the potential energy at the same extreme conformations have been estimated for the individual common residues (with the exception of proline) as 0 *kcal/mol* for the lowest-energy, 6 *kcal/mol* for the local minimum and 16 *kcal/mol* for the transition state. Although these values are somewhat less than for alanine residue but by the same reason they are more comfortable for the conformational transitions between the allowed conformations with negative and positive values of $\phi$ angle. These values of the energy therefore were used in the following estimations.

The above values of the potential energy and simple calculations of the rate and equilibrium constants of the corresponding conformations by the known formulas $K = exp\ (-H/RT)$ and $\tau = \tau_o{*}K$ strongly prove that in native protein spatial structure nonglycine residues should have an allowed conformation with negative torsion angle $\phi$ from both kinetic and thermodynamic points of view. In the formulas, $K$ is the equilibrium constant, $\Delta H^\circ$ is the energy difference and $\tau$ is the rate constant of the transitions of two conformations 1 and 2, $RT$ = 0.5961 *kcal/mol* at 27°C and $\tau_o$ is $10^{-12}$ *s*. The estimations are as follows.

For the transition state and lowest energy conformations, $\Delta H^\circ \approx$ 16 *kcal/mol* as above, $K = 4.54{*}10^{11}$ and $\tau$ = 0.454 *s*. $\tau$ is the residence time of the lowest energy conformation, the rate constant of the transition state or the time required to transit to the allowed conformations with positive values of . It should be remembered here that a polypeptide chain is synthesized in and starts folding from the same conformation for all the residues because of the stereospecificity of the enzymatic reaction in the peptidyltransferase center of the ribosome. The angle $\phi$ for this initial conformation should be negative as its value is limited in the interval of –80° to –40° for the proline residue [37,38]. The right-handed $\alpha$-helix (~–60°,~–50°) most likely corresponds to this conformation [39,40]. The value of 0.454 *s* for $\tau$ can be compared to the typical times of the conformational alterations in organic molecules of $10^{-12}$ – $10^{-7}$ *s* [41-43] and for the formations of -helices, -sheets, turns and compact states in unfolded polypeptide of $10^{-7}$ – $10^{-2}$ *s* [43-46]. The events listed happen obviously much faster than 0.454 *s*, *e.g.* either $\alpha$–helix, $\beta$–sheet, turn and compact state has to be molded in a nascent polypeptide before a nonglycine residue might transit at the 0.454 *s* rate constant from the allowed region with negative angles $\phi$ to the region with positive $\phi$ since the moment when the biosynthesis of the chain begins.

The above data suggest that the activation barrier should be noticeably lower than 16 *kcal/mol* for the conformational transition of a nonglycine residue to occur from the allowed region with negative values of $\phi$ to the region

with positive $\phi$. This could be preferably attained at the expense of significant deformations of the valence angles flanking the $NC^{\alpha}$ bond of the residue. Such effects may take place in dipeptides according to the *ab initio* quantum-mechanical calculations with optimization of the geometry [47,48]. In particular, in glycine dipeptide the lowering of the barrier from 18.7 to 12.3 *kcal/mol* is achieved at the expense of the simultaneous widening of the bond angles $NC^{\alpha}C$ from 110° to 118.5° and $CNC^{\alpha}$ from 123° to 131° [47]. Though the 12.3 *kcal/mol* energy is even high enough for conformational alterations, a deformation of a backbone valence angle by about 10° will hardly occur in a highly constrained and tightly packed unperturbed polypeptide chain. Such a deformation will be relaxed and compensated on the adjoining valence angles first and also will lead to unexpected closest contacts between the neighboring nonbonded atoms.

The data and speculations above are related to the vacuum medium. Many factors will exert influence on the conformational equilibrium and reorganizations of molecules in aqueous and condensed media. Among them are possible formations of intra- and intermolecular hydrogen bonds, intermolecular interactions, the effect of the environment on rotational mobility, steric hindrances in the limited free space [49]. These factors will hamper and make even more difficult the realization of the transition discussed above.

The equilibrium and rate constants also can be estimated for the conformations of the transition state and local minimum nevertheless, although the conformations divided by a high activation barrier will coexist separately for a long time independently of the difference in the energies [50]. For these, $\Delta H^{\circ} \approx 10$ *kcal/mol*, $K = 1.93*10^{7}$ and $\tau = 1.93*10^{-5}$ *s*. $\tau$ is the residence time of the local minimum or the time required to transit from this minimum backward to the allowed region with negative values of angle $\phi$, and it is much less than 0.454 *s* required for the transition from the lowest energy state $2.35*10^{4}$ times. Hence, the probability of a nonglycine residue to reside in an allowed conformation with positive angle is $4.25*10^{-5}$ $(1/(2.35*10^{4}))$. The main deduction from the above is that nonglycine residues in protein spatial structure should have an allowed conformation with negative backbone torsion angle $\phi$; it is unlikely for them as to get as well as reside in a conformation with positive $\phi$ angle from both kinetic and thermodynamic points of view.

## 3.2 The Crystal Structure Data on Proteins Evince: Nonglycine Residues with Positive Torsion Angle $\phi$ should be distinguished as Outliers

### 3.2.1 Revision of the conformations of nonglycine residues in the 'old' protein structures

For the high resolution 195 'old', deposited in the PDB by 1992 protein structure models, revisions of the signs of the backbone torsion angles $\phi$ of the equivalent residues made proven the following general inferences (the PDB codes of structures and the results can be found in Appendix).

The sign of the backbone torsion angle $\phi$ of nonglycine residues in the structure models of a protein does not change with changes of the functional state of protein and medium (binding of a ligand or inhibitor, mutation, crystallization conditions, crystalline medium, crystalline form, *etc.*).

The torsion angles $\phi$ of the same, equivalent or homologous nonglycine residues have the same sign in the structure of identical subunits of oligomeric proteins and of the same protein of different origins.

The number of nonglycine residues with positive $\phi$ decreases with the improvement of the resolution and the quality of determination and refinement of the protein structure.

A relatively large amount of nonglycine residues with positive $\phi$ in the protein structure may be a simple indicator of local inaccuracies such as abnormally short distances between the nonbonded atoms, unusual valence bond lengths and bond angles and poor stereochemistry.

### 3.2.2 A review of the conformations of nonglycine residues in the highest resolution protein structures

The PDB codes of 182 highest resolution protein structures analyzed and the results on the occurrences of nonglycine residues in conformations with positive backbone angle $\phi$ in these structures can be found in Appendix in Table 1. According to the results, nonglycine residues with positive $\phi$ are lacking in 16 of 182 structures and such residues make less than 2% of nonglycine residues in other 59 structures. In all 182 structures, 28287 non-terminal nonglycine

residues are counted; 716 of these (2.5%) with positive $\phi$ are registered. Fractions with positive $\phi$ were analyzed for the individual common residues. Table 1 presents the results, which also lists nonglycine residues with positive $\phi$ that have either nontypical molecular geometry or stereochemical parameters or negative value of $\phi$ in some other structure model of the corresponding same proteins.

The revisions disclosed that of 716 with positive $\phi$ nonglycine residues present in all structures, 41 (5.7 %) have either nontypical bond lengths or bond angles or unexpected values for $\phi$, $\psi$ or torsion angles. Other 113 residues (15.6%) had the conformation with a negative $\phi$ angle in some another ≤ 2.0 Å resolution structure model of the corresponding proteins. It will be justified to exclude these both types 154 residues from the statistics. The portion of nonglycine residues with positive $\phi$ constituted in all structures on average less of 2%. With positive $\phi$ registered no Pro residues, 4 Val residues of 2219 (0.2%), 4 Ile of 1594 (0.3%), 7 Thr of 1994 (0.3%), 18 Leu of 2362 (0.8%), and 5 Trp of 466 (1.1%) residues (Table 1). An identification of these residues is given in Table 2. For the other individual common residues, the fraction with positive $\phi$ obtained for His 4.3%, for Asp 4.8%, for Asn 13.1%, and for rest ten type common residues from 1.3 to 2.3% (visually, in Appendix Fig. 1 displays the Ramachandran plots of the total nonglycine residues, His, Asp and Asn and the rest 16 type nonglycine residues).

It has been shown in this study that for nonglycine residues, the lowest energy conformation with negative value of backbone torsion angle $\phi$ is favorable than that with positive by about 6 *kcal/mol* and these conformations are separated by nearly 16 *kcal/mol*, *i.e.* almost comparable to the peptide bonds trans-to-cis transition barrier of around 18 *kcal/mol*, activation barrier. From these, the probability of $4.25*10^{-5}$ to reside and the rate constant of 0.454 *s* to transit to the conformations with positive $\phi$ are estimated. The data, also the consideration of the biogenesis of proteins and typical times of $10^{-7}$ – $10^{-2}$ *s* for the formation of secondary structure and compact states in polypeptides, evince that it is unlikely for nonglycine residues both to get and to reside in a conformation with positive $\phi$ from both kinetic and thermodynamic points of view. Therefore, nonglycine residues in protein spatial structure should most likely have an allowed conformation with a negative value of backbone torsion angle $\phi$. The deduction is the main fundamental result of this study.

The deduction made is believed to be supported by the crystal structure data on proteins. Above all, it explains rationally the common observations of only rare occurrence of nonglycine residues in conformations with positive torsion angle $\phi$ in protein crystal structures. The current analysis of the highest resolution 182 largely nonhomologous protein structures has detected on average 2% with positive $\phi$ of the total nonglycine residues. The same result obtained also in other studies [28,51]. The statistics persuades to that a conformation with positive value of angle $\phi$ is certainly unique and exceptional for nonglycine residues in proteins. Moreover, such a conformation may be outlier, taking into account that the procedures of protein structure determination (phase determination, electron density map interpretation, fitting a model in map, rebuilding and refining the model) are to some extent subjective [1-3]. In addition, it has been revealed in this study that the relatively large amount of nonglycine residues with positive value of $\phi$ will be a simple indicator of the lack of accuracy in the protein structure model. It should be also remembered that the residues with positive $\phi$ in protein structures are usually observed in the reverse turns on the exteriors of the globule and hence their coordinates may be determined not accurate enough. Thus nonglycine residues with positive angle $\phi$ in protein structure may be supposed as outliers having a dubious conformation to be a result of errors introduced upon structure solution.

This study puts forward the throughout reinvestigations of protein structures for coordinate errors in the segments including nonglycine residues with positive $\phi$ angle (at least of the backbone atoms producing the angle $\phi$). With account that in the structures analyzed here with positive detected only 0.2% of Val, 0.3% of Ile, 0.3% of Thr, 0.8% of Leu, and 1.1% of Trp residues compared to the other type residues (Table 1), reinvestigations of these residues (listed in Table 2) might be of top-priority. A relatively great fraction residues with positive $\phi$ were detected for His (4.3%), Asp (4.8%) and Asn (13.1%), while. In this regard, a distinctive feature of these residues may be emphasized that their side chain has a conjugative-bounded heteroatom in $\delta$ position ($O^{\delta}$ – Asp and Asn and $N^{\delta}(H)$ – His).

**Table 1. Fractions of the individual common and total nonglycine residues with positive $\phi$ in 182 highest resolution protein structures**

| 1 | 2 | 3 | 4 | 5 | 6 |
|---|---|---|---|---|---|
| Pro | 1420 | 0 | 0.0 | 0 | |
| Ile | 1595 | 5 | 0.3 | 1 | 154 (3NOQ): 3NOV, 3NOO, 3NOV. |
| | | 4 | 0.2 | 1* | *194 (3DHA). |
| Val | 2220 | 5 | 0.2 | 1 | 17 (2CGA): 5CHA, 2AYW, 1TPP, 1TGB. |
| | | 4 | 0.2 | 0 | |
| Thr | 1998 | 11 | 0.6 | 3 | 133 (5CPA): 1ELL, 1M41, 1YME, 3FVL, 3HLP; 151 (2CGA): 5CHA; 217 (6LDH): 1LDM. |
| | | 8 | 0.4 | 0 | |
| Trp | 467 | 6 | 1.3 | 1 | 89 (3IP0): 1G4C. |
| | | 5 | 1.1 | 1* | *90 (8FAB). |
| Leu | 2366 | 22 | 0.9 | 6 | 74 (1FX1): 1J8Q; 327 (6LDH): 1LDM; 64 (1VL9): 1G4I, 1BP2, 1P2M, 1KVW; *95 (2PKA); *3 (1LH1); *20 (2CI2); *99 (2XOD); *90 |
| | | 17 | 0.7 | 4* | (3DFR). |
| Phe | 1158 | 16 | 1.4 | 1 | 45 (2XOD): 2X2P, 2XOE |
| | | 15 | 1.3 | 0 | |
| Met | 563 | 13 | 2.3 | 2 | 180 (1RTQ): 3B35 (Ala); 145 (1HJ8): 1NTP, 1TPA, 1TPO, 1TGB, 1TGS. *69 (1N9B); *69 (1M40). |
| | | 11 | 2.0 | 2* | |
| Cys | 665 | 13 | 2.0 | 3 | 334 (2CPP): 2LQD (NMR); 341 (2XFR): 1B1Y, 1Q6C; 157 (3KFF): 2LB6 (176). *204 (2VHK); *3 (1VBW); *69 (1YLJ). |
| | | 10 | 1.5 | 3* | |
| Ala | 2734 | 51 | 1.9 | 16 | 38 (1FX1): 1J8Q; 2 (1LH1): 2GDM; 92 (8FAB): 8FAB (B chain); 185 (2CGA): 1TGN; 207 (1BYI): 1DTS; 12 (3IP0): 1G4C (B); |
| | | 35 | 1.3 | 3* | 151(3IP0): 1G4C (A); 221 (1HJ8): 1TGN, 2TGD, 2CGA; 221 (2AYW): 1TGN, 2TGD, 2CGA; 39 (1AHO): 1SN1; 217 (1PQ7): 1TGN, 1HJ8; 172 (1M40, 1N9B, 1YLJ): 3B3X, 1W7F. 50 (2I4A): 1XWC, 2E0Q; *35 (351C); *147 (1GD1); *238 (2ZPM). |
| Lys | 1755 | 46 | 2.6 | 8 | 54 (2PVB): 1B9A; 106 (3WRP): 2OZ9, 1WRP; 221, 328 (6LDH): 1LDM; 82 (2CTS): 3ENJ; 146 (1P1X): 1JCJ, 1JCL; 173 (2QXI): |
| | | 38 | 2.2 | 2* | 3BSQ (167); 117 (2CE2): 1BK9; *252 (3KS3); *176 (1EB6). |
| Glu | 1641 | 28 | 1.7 | 1 | 31 (2R31): 2ZD2; *208 (1BYI). *239 (2CTS); *373 (1GWE); *35 (2A6Z); *123 (1LKK). |
| | | 27 | 1.6 | 5* | |
| Ser | 2172 | 55 | 2.5 | 14 | 107 (3WRP): 2OZ9, 1WRP; 134 (5CPA): 1BAV, 1M41, 3HLP; 2 (2CTS): 3ENJ; 298 (2JHF): 1JU9, 1QLJ, 1YE3 (A chain); 142 |
| | | 41 | 1.9 | 5* | (1ZK4): 1NXQ, 1ZK0, 1ZK3; 193 (2XFR): 2XFF, 2XG9, 2XGB; 74 (3E4G): 3E2J; 56 (1ZZK): 1ZZI; 43 (2PND): 2ICC, 2ICE, 2ICF; 13 (3IP0): 1G4C (B), 1Q0N; 52 (2F01): 1SLE, 1PTS; 202 (2AYW): 2CGA (Lys); *3 (2CCY); *2 (2RHE); *8 (3EBX); *125 (3D1P); *103 (3NOQ). |
| Arg | 1228 | 29 | 2.4 | 2 | 241 (1M40): 1N9B; 35 (1GQV): 1H1H (Trp35), 1QMT (Trp35); *109 (1UFY). |
| | | 27 | 2.2 | 1* | |
| Tyr | 1069 | 32 | 3.0 | 7 | 98 (1FX1): 1J8Q; 244 (6LDH): 1LDM; 105 (1N9B): 1YLJ, 3B3X, 1W7F; 105 (1M40): 1YLJ, 3B3X, 1W7F; 241 (1YLJ): 1N9B (Arg); |
| | | 25 | 2.3 | 1* | 25 (1HJ8): 1TGS (Asn); 97 (3KFF): 2LB6 (116). *172 (3RP2). |
| Gln | 1194 | 31 | 2.7 | 6 | 100 (6LDH): 1LDM; 197 (1N9B): 3N4I, 2G2U; 85 (3BWH): 3QJI, 3S9Q, 3SJ6; 185 (3F1L): 3F1K; *60(1AEC). |
| | | 25 | 2.1 | 1* | |

| 1 | 2 | 3 | 4 | 5 | 6 |
|---|---|---|---|---|---|
| His | 695 | 34 | 4.9 | 4 | 99 (2QXI): 3BSQ (95); 37 (3D1P): 1H4M (40); 3 (2I4A): 3E0Q (His39). *3 (3GOE); *297 (1MJ5). |
| | | 30 | 4.3 | 2* | |
| Asp | 1848 | 101 | 5.5 | 13 | 129 (9WGA): 2UVO (B chain); 267 (1N9B): 1YLJ (Thr266); 254 (1M40): 1YLJ (Gln); 243 (3KS3): 2CAB (His); 151 (1NLS): 2CNA; |
| | | 88 | 4.8 | 4* | 97 (3HGP): 2DE9, 3EST; 32 (3NOQ): 3NOO; 63 (2IIM): 1H92 (NMR); 85 (3KFF): 2LB6( 104); 12 (3F1L): 3F1K; 223 (6LDH): =7°; *276 (6LDH); *185 (1AEC); *174(1TON); *25(2VHK). |
| Asn | 1476 | 217 | 14.7 | 24 | 67 (1DY5): 1RSM, 3RN3, 3I6J; 51 (1KWF): 1CEM; 188 (1LKK): 1CWD (66); 75 (1LZ1): 1GB9, 1GE1, 1ILZ, 1LMT; 69 (1NLS): |
| | | 193 | 13.1 | 6* | 2EF6, 2P37; 36 (1PQ7): 1HJ8, 1TGB, 3PTN; 220 (1PQ7): 1TGN (223); 44 (1RNT): 4BIR; 24 (1VL9): 3OSH, 3NJU, 3MLM (Asn); 170 (1X8Q): 3MVF; 25 (2AYW): 1TGS; 223 (2AYW): 1TGN; 26 (2CE2): 1BKD; 150 (2CGA, A chain): 2CGA (B); 192 (2GGC): 1XNZ, 2EVC, 2GG0, 2Q92; 98 (2PAB): 1DVS, 1E3F, 1Z7J; 223 (2QXI): 216 (3BSQ); 74 (2VB1): 2BLX, 2BPU, 6LYZ; 179 (2XU3): 2NQD, 2YJ8; 173 (3EA6): 2NTT; 161 (3F1L): 3F1K; 218 (6LDH): 1LDM; 9 (9WGA): 2X52; *209, *212 (1BYI); *2 (1ZK4); *95 (2PKA); *62(1UCS), *276(2PWA). |
| Non-Gly | 28287 | 716 | 2.5 | 113 | |
| | | 603 | 2 | 41* | |
| Gly | 2800 | 1616 | 58.9 | | |

*Note: For every residue, columns present: 1, the name and 2, total number of residue; 3 to 5 correspondingly, in the first line: the number of residues with positive $\phi$, the percentage fraction of residues with positive $\phi$, the number of residues with positive $\phi$ which are with negative $\phi$ in some other structure of the same proteins; in the second line: the number of residues with positive $\phi$ except the residues that are with negative $\phi$ in some other structure of the same proteins, the percentage fraction of residues with positive $\phi$ except the residues that are with negative $\phi$ in some other structure of the same proteins, the number of residues with positive $\phi$ that have nontypical geometry or unexpected values for $\phi$, $\psi$ or $\omega$ angles (marked by "*"); column 6: the identifications of the residues with positive $\phi$: which have negative $\phi$ in some other structure of the same protein or nontypical bond lengths, bond angles or unexpected values for $\phi$, $\psi$ or $\omega$ angles. In the list, on the left of each semicolon are the residue number in the chain and the PDB code of the structure nearby in parentheses. On the right of each semicolon is given the PDB code(s) of other structure model(s) of the same protein in which the residue is with negative $\phi$. Residues with unusual geometry or dubious stereochemical parameters are marked by "*".The penultimate line "Non-Gly" presents the data on the total nonglycine residues. NMR is Nuclear Magnetic Resonance*

**Table 2. A list of Ile, Val, Thr, Leu, and Trp residues with positive angle in 182 structures**

| | |
|---|---|
| Ile | 99 (1HJ8), 30 (1REI), 99 (2CGA), 194 (3DHA) |
| Val | 237 (1GD1), 22 (1GWE), 69 (3BWH), 59 (3EBX) |
| Trp | 80 (1UNQ), 191 (2DDX), 183 (2FVY), 300 (2XFR), 90 (7FAB) |
| Thr | 43 (1CEX), 14 (1G66), 84 (1UZV), 157 (1X8Q), 103 (2CWS), 83 (2PND), 102 (2V8T) |
| Leu | 60 (1F94), 230 (1NLS), 19 (1R2M), 155 (1RTQ), 45, 99 (2AYW), 223 (2DDX), 119 (2G58), 141 (2JHF), 126 (2V1M), 99 (2XOD), 223 (3DK9), 203 (3KS3), 124 (3F7L) |

*Note: For every item in the list in column 2, figure is the number of the residue in the polypeptide chain and nearby in the parentheses is the PDB code of the structure*

The reliable conformation analyses of peptide models of these residues independently together with the reinvestigation of the segments involving such with positive $\phi$ residues in the respective structures might be wholesome and promising.

In the approximation of all *trans*-peptide bonds, a conformation of polypeptide chain is characterized by a set of values of $\phi$ and $\psi$ backbone torsion angles. This study sets that in polypeptides all 19 types of common nonglycine residues possess by one of these two backbone angles, by $\phi$, depleted flexibility by half (most likely as early as ever since from the biosynthesis); their conformational alterations will take place only in the allowed regions with negative values of angle of $\phi$ of $(\phi,\psi)$ torsion angles area. This feature might be a plausible determinative for fast and efficient folding of proteins.

## 4. CONCLUSION

Nonglycine residues in native protein spatial structure should most likely have an allowed conformation with a negative value of backbone torsion angle $\phi$; it is unlikely for them both to get and to reside in a conformation with positive $\phi$ from both kinetic and thermodynamic points of view. Residues with positive $\phi$ angle in a protein structure are suggested as outliers having a dubious conformation to be a result of errors introduced upon structure solution and should be inspected thoroughly for coordinate errors.

The results of this study may be important in biophysics, bioinformatics and structural biology, in elucidating the stability, folding problem and principles of spatial structure organization of proteins and can be employed for further re-refinement of protein structure models and in protein structure solution by X-ray crystallography.

## COMPETING INTERESTS

Author has declared that no competing interests exist.

## REFERENCES


1. Blundell TL, Johnson LN. Protein crystallography. New York: Academic Press; 1976.
2. Richardson JS. The anatomy and taxonomy of protein structure. Adv in Prot Chem. 1981;34:167–339.
3. Drenth J. Principles of protein X-ray crystallography. Springer: New York; 2007.
4. Ilari A, Savino C. A practical approach to protein crystallography. Methods Mol Biol. 2017;1525:47–78.
5. Bränden CI, Jones TA. Between objectivity and subjectivity. Nature (London). 1990;343:687–689.
6. Janin J. Errors in three dimensions. Biochimie. 1990;72:705–709.
7. Vriend G, Sander C. Quality control of protein models: Directional atomic contact analysis. J Appl Crystallog. 1993;26:47–60.
8. Hooft RWW, Sander C, Vriend G, Abola E. Errors in protein structures. Nature (London). 1996;381:272.
9. Kleywegt GJ, Jones TA. Where freedom is given, liberties are taken. Structure. 1995;3:535–540.
10. Kleywegt GJ. Validation of protein crystal structures. Acta Cryst. 2000;D56:249–265.
11. Penders B, Horstman K, Vos R. Proper science in moist biology. EMBO Reports. 2007;8:613.
12. Borrell B. Fraud rocks protein community. Nature (London). 2009;462:970.
13. Ramachandran GN, Ramakrishnan C, Sasisekharan V. Stereochemistry of polypeptide chain configurations. J. Mol. Biol. 1963;7:95–99.
14. Brant DA, Schimmel PR. Analysis of the skeletal configuration of crystalline hen egg-white lysozyme. Proc Natl Acad Sci USA. 1967;58:428–435.
15. Ramachandran GN, Sasisekharan V. Conformation of polypeptides and proteins. Adv Prot Chem. 1968;23:283–437.
16. Scheraga HA. Calculations of conformations of polypeptides. Adv Phys Org Chem. 1968;6:103–184.
17. Morris AL, MacArthur MW, Hutchinson EG, Thornton JM. Stereochemical quality of protein structure coordinates. Proteins: Struct Funct Genet. 1992;12:345–364.
18. Laskowski RA, MacArthur MW, Moss DS, Thornton JM. PROCHECK: A program to check the stereochemical quality of protein structures. J Appl Cryst. 1993;26:283–291.
19. Hooft RW, Sander C, Vriend G. Objectively judging the quality of a protein structure from a Ramachandran plot. Comput Appl Biosci. 1997;13(4):425-430.

20. Kleywegt GJ, Jones TA. Phi/Psi-chology: Ramachandran revisited. Structure. 1996;4:1395–1400.
21. Lovell SC, Davis IW, Arendall WB 3rd, de Bakker PIW, Word JM, Prisant MG, Richardson JS, Richardson DC. Structure validation by C$\alpha$ geometry: $\phi$, $\psi$ and C$\beta$ deviation. Proteins: Struct Funct Genet. 2003;50:437–450.
22. Chen VB, Arendall WB 3rd, Headd JJ, Keedy DA, Immormino RM, Kapral GJ, Murray LW, Richardson JS, Richardson DC. MolProbity: All-atom structure validation for macromolecular crystallography. Acta Cryst. 2010;D66:12–21.
23. Read RJ, Adams PD, Arendall WB 3rd, Brunger AT, Emsley P, Joosten RP, Kleywegt GJ, Krissinel EB, Lütteke T, Otwinowski Z, Perrakis A, Richardson JS, Sheffler WH, Smith JL, Tickle IJ, Vriend G, Peter H, Zwart PH. A new generation of crystallographic validation tools for the protein data bank. Structure. 2011;19: 1395–1412.
24. Bernstein FC, Koetzle TF, Williams GJB, Meyer EF Jr, Brice MD, Rodgers JR, Kennard O, Shimanouchi T, Tasumi M. The protein data bank: A computer based archival file macromolecular structures. J Mol Biol. 1977;112:535–542.
25. Berman HM, Henrick K, Nakamura H, Markley JL. The worldwide Protein Data Bank (wwPDB): Ensuring a single, uniform archive of PDB data. Nucl Acids Res. 2007;35:D301–D303.
26. Hollingsworth SA, Karplus PA. A fresh look at the Ramachandran plot and the occurrence of standard structures in proteins. BioMol Concept. 2010;1:271–283.
27. Zhou AQ, O'Hern CS, Regan L. Revisiting the Ramachandran plot from a new angle. Prot Sci. 2011;20:1166–1171.
28. Kalmankar NV, Ramakrishnan C, Balaram P. Sparsely populated residue conformations in protein structures: Revisiting "experimental" Ramachandran maps. Proteins. 2014;82:1101–1112.
29. Krieger E, Vriend G. New ways to boost molecular dynamics simulations. J. of Comput Chem. 2015;36:996–1007.
30. Singh A, Kaushik R, Mishra A, Shanker A, Jayaram B. ProTSAV: A protein tertiary structure analysis and validation server. BBA – Proteins and Proteomics. 2016; 1864:11–19.
31. Momany FA, McGuire RF, Burgess AW, Scheraga HA. Energy parameters in polypeptides, VII: Geometric parameters, partial atomic charges, nonbonded interactions, hydrogen bond interactions, and intrinsic torsional potentials for the naturally occurring amino acids. J Phys Chem. 1975;79:2361–2380.
32. Vasquez M, Nemethy G, Scheraga HA. Conformational energy calculations of polypeptides and proteins. Chem Rev. 1994;94:2183–2239.
33. Engh RA, Huber R. Accurate bond and angle parameters for X-ray protein structure refinement. Acta Cryst. 1991;A47:392–400.
34. Basharov MA, Vol'kenshtein MV, Golovanov IB, Ermakov GL, Nauchitel' VV, Sobolev VM. Bond-bond interactions. A simple relationship for estimating the energy of a bond–bond interaction. J Struct Chem. 1984;25:26–29.
35. Basharov MA. Modified method of fragment-fragment interactions for studying intra- and intermolecular interactions. Russ J Phys Chem. 1995;69:1284–1288.
36. Basharov MA. The internal rotational barriers about NC and CC backbone bonds of polypeptides. Eur Biophys J. 2012;41:53–61.
37. DeTar D-LF, Luthra N. Conformations of proline. J Am Chem Soc. 1977;99:1232–1244.
38. Peters D, Peters J. Quantum theory of the structure and bonding in proteins. The proline dipeptide. J Mol Struct. 1981;85(9):257–265.
39. Lim V, Spirin AS. Stereochemical analysis of ribosomal transpeptidation. J Mol Biol. 1986;188:565–574.
40. Bhushan S, Gartman M, Halic M, Armache J-P, Jarasch A, Mielke T, Berninghausen O, Wilson DN, Beckman R. Helical nascent polypeptide chains visualized within distinct region of the ribosomal exit tunnel. Nat Struct Mol Biol. 2010;17:313–317.
41. Schwarz G. On the kinetics of the helix-coil transition of polypeptides in solution. J Mol Biol. 1965;11:64–77.
42. Schwarz G. General theoretical approach to the thermodynamic and kinetic properties of cooperative intramolecular transformations of linear biopolymers. Biopolymers. 1968;6:873–897.

43. Eigen M. Dynamics of conformational changes in helical macromolecules. Chim Phys. 1968;65:53.
44. Williams S, Causgrove TP, Gilmanshin R, Fang KS, Callender RH, Woodruff WH, Dyer RB. Fast events in protein folding: Helix melting and formation in a small peptide. Biochemistry. 1996;35:691–697.
45. Eaton WA, Munoz V, Thompson PA, Chan CK, Hofricher J. Fast events in protein folding. Curr Opin Struct Biol. 1997;7:10–14.
46. Sosnick TR, Shtilerman MD, Mayne L, Englander SW. Ultrafast signals in protein folding and the polypeptide contracted state. Proc Natnl Acad Sci USA. 1997;94:8545–8550.
47. Hiller IH, Robson B. Conformational behavior of the architectural units of peptides and proteins. Assessment of current understanding by ab initio quantum mechanical methods and refinement of the dipeptide energy surface. J Theor Biol. 1979;76:83–98.
48. Head-Gordon T, Head-Gordon M, Frisch MJ, Brooks III CL, Pople JA. Theoretical study of blocked glycine and alanine peptide analogues. J. Am. Chem. Soc. 1991;113:5989–5997.
49. Burshtein AI. Molecular-kinetic aspects of the chemical physics of condensed states. Advan in Chemistry (USSR) 1978;XLVII: 212–234.
50. Volkenstein MV. Molecular Biophysics. New York, London: Academic Press Inc.; 1978.
51. Fitzkee NC, Fleming PJ, Gong H, Panasik N Jr, Street TO, Rose GD. Are proteins made from a limited parts list? Trends Biochem Sci. 2005;30:73–80.

## APPENDIX

**PDB codes of ≤ 2.0 *Å* resolution 195 protein structures:**

1ACX, 1AEC, 1CAC, 1CCR, 1CHO, 1CRN, 1CSE, 1CYP, 1ECA, 1ECD, 1ECN, 1ECO, 1FX1, 1GD1, 1GP1, 1HDS, 1LH1, 1LH2, 1LH3, 1LH4, 1LH5, 1LH6, 1LH7, 1L01, 1L02, 1L03, 1L04, 1L05, 1L06, 1L07, 1L08, 1L09, 1L10, 1L11, 1L12, 1L13, 1L14, 1L15, 1L16, 1LDM, 1LYZ, 1LZ1, 1LZT, 1MB5, 1MBA, 1MBD, 1MBN, 1MBO, 1NTP, 1NXB, 1OVO, 1PAZ, 1PPD, 1PPT, 1REI, 1RN3, 1RNS, 1RSM, 1RSN, 1RNT, 1SGC, 1SGT, 1TGB, 1TGC, 1TGN, 1TGS, 1TGT, 1TON, 1TPA, 1TPO, 1TPP, 1UBQ, 1WRP, 2ACT, 2ALP, 2APR, 2AZA, 2C2C, 2CAB, 2CCY, 2CDV, 2CGA, 2CHA, 2CI2, 2CNA, 2CPP, 2CTS, 2CYP, 2FB4, 2FD1, 2FOX, 2GCA, 2GCH, 2GRS, 2HMQ, 2HMZ, 2HHB, 2LH1, 2LH2, 2LH3, 2LH4, 2LH5, 2LH6, 2LH7, 2LHB, 2LYM, 2LYZ, 2LZM, 2MHB, 2MBN, 2OVO, 2PAB, 2PCY, 2PKA, 2PRK, 2PTC, 2PTN, 2RNS, 2SEC, 2TGA, 2TGP, 2TGT, 2RHE, 2SGA, 2SN3, 2SNS, 2SOD, 351C, 3APP, 3C2C, 3CPA, 3CYT, 3DFR, 3EBX, 3EST, 3GRS, 3HHB, 3LYM, 3LYZ, 3MBN, 3OVO, 3PCY, 3PTN, 3PTB, 3PTP, 3RP2, 3SGB, 3TLN, 3TPI, 3WRP, 451C, 4CHA, 4CPV, 4CYT, 4DFR, 4FD1, 4HHB, 4GCR, 4LYZ, 4LZM, 4OVO, 4PCY, 4PTP, 4RXN, 4TNC, 4PTI, 5CHA, 5CPA, 5CPV, 5CYT, 5EBX, 5FD1, 5LYZ, 5LZM, 5NLL, 5PTI, 5RXN, 5TNC, 5PCY, 6CHA, 6LDH, 6LYT, 6LYZ, 6LZM, 6LYZ, 6PCY, 6PTI, 6TMN, 7FAB, 7RXN, 8FAB, 8LYZ, 8TLN, 9PAP, 9WGA.

**The results of the analyses of ≤ 2.0 *Å* resolution 195 protein structure models**

*A: The sign of the backbone torsion angle $\phi$ of nonglycine residues in the structure models of a protein does not change with changes of the functional state of protein and medium (binding of a ligand or inhibitor, mutation, crystallization conditions, crystalline medium, crystalline form, etc.).* Evidence for this is provided by the examples below, where next to the name of protein are given in the parentheses the PDB codes of structure models of that protein in different functional state or medium conditions. They are the structures of: erythrocruorin (1ECA, 1ECD, 1ECN, 1ECO), myoglobin (1MBN, 2MBN, 3MBN, 1MBO), leghemoglobin (1LH1 to 1LH7, 2LH1 to 2LH7), hemerythrin (2HMQ, 2HMZ), cytochrome C (3CYT, 4CYT, 5CYT), cytochrome C2 (2C2C, 3C2C), cytochrome C551 (351C, 451C), cytochrome C peroxidase (1CYP, 2CYP), plastocyanin (3PCY, 4PCY, 5PCY, 6PCY), carboxypeptidase A (3CPA, 5CPA), lysozyme phage T4 (1L01 to 1L16, 2LZM, 4LZM, 5LZM, 6LZM), papain (9PAP, 1PPD), thermolysin (8TLN, 6TMN), trypsin inhibitor (4PTI, 5PTI, 6PTI), -trypsin (1TPO, 3TPO, 3PTN, 1TPP, 3PTP, 3TPT, 1TPA), -chymotrypsin A (2CHA, 6CHA, 1CHO), and trypsinogen (1TGC, 2TGT). A few exceptions from the tendency can be found below.

*B: The torsion angles $\phi$ of the same, equivalent and homologous nonglycine residues have the same sign in the identical subunits of oligomeric proteins and of the same protein of different origins.* The examples are the structures: 9WGA of agglutinin, 2AZA of azurin, 2CCY of cytochrome C, 1REI of immunoglobulin, 2PKA of kallikrein A, 3RP2 of protease II, and 4CHA of $\alpha$-chymotrypsin, all of them consisting of two identical subunits, 4HHB of hemoglobin consisting of two pairs of identical subunits, 2HMQ of hemerythrin and 1OVO of ovomucoid 3rd domain both of them consisting of four identical subunits, 4TNC of chicken and 5TNC of turkey troponin C, 5RXN of *Clostridium Pasteurianum* and 7RXN of *Desulfovibrio Vulgaris* rubredoxin, and 1OVO of *Japanese quail* and 2OVO of *Silver pheasant* ovomucoid 3rd domain. Exceptions from the tendency are structures 2PAB of prealbumin, 2CGA of chymotrypsinogen A, 1HDS of deer sickle hemoglobin S, and 2SOD of superoxide dismutase. Structure 2PAB contains nonglycine residues with positive $\phi$ 4 in the first of two identical subunits and 3 in the second subunit. Of two identical subunits of structure 2CGA the first has 7 nonglycine residues with positive $\phi$ and such residues are 10 in the second subunit. Angle $\phi$ of a noticeable number of identical nonglycine residues has different sign in two identical pairs of subunits of structure 1HDS and in four identical subunits of structure 2SOD.

The above inferences confirmed also by enormous examples from the PDB testify to the invariability of the sign of torsion angle $\phi$ of the equivalent residues in different structure models of the same proteins. Incidentally, the inferences are also true for glycine residues.

*C: The number of nonglycine residues with positive $\phi$ in the 3D structure decreases with the improvement of the resolution and the quality of determination and refinement of the structure.* The tendency is confirmed by the following examples in particular. Nonglycine residues with positive $\phi$ are: in the flavodoxin obsolete structures at 1.9 *Å* resolution (3FXN) 6 and at 1.8 *Å* (4FXN) 5 and 1.75 *Å* resolution superseded structure (5NLL) 3, in human hemoglobin structure at 2.1*Å* (1HHO) 5 and at 1.5 *Å* (1THB) 2, in lactate dehydrogenase obsolete structure (4LDH) 33 and superseded structure (6LDH) 16 both they at 2.0 *Å*, in rubredoxin obsolete structure (4RXN) 2 and superseded structure (7RXN) 0 both they at 1.5 *Å*, in Trp-repressor domains obsolete structure at 2.0 *Å* (3WRP) and superseded structure at 1.65 *Å* (2OZ9) 1 (deposited in the PDB in 2007), in glutathione reductase 2.0 *Å* resolution obsolete structure (2GRS) 24 and superseded structure at 1.54 *Å* (3GRS) 12, in Fab New immunoglobulin obsolete structure 3FAB 49 and superseded structure 8FAB 16 both they at 2.0 *Å*, in Kol Fab immunoglobulin obsolete structure 1FB4 at 2.0 *Å* 17 and superseded structure 2FB4 at 1.9 *Å* 11, in lamprey hemoglobin obsolete structure 1LHB 6 and superseded structure 2LHB 1 both they at 2.0 *Å*, in parvalbumin obsolete structure 3CPV at 1.85 *Å* 4 and superseded structure 4CPV at 1.5 *Å* 3, in ribonuclease S obsolete structure 1RNS 10 and superseded structure 2RNS 1 both they at 1.6 *Å*. The following examples were exceptions from the tendency. Nonglycine residues with positive $\phi$ are in the structure: of lactate dehydrogenase at 2.1 *Å* (1LDM) 10 and at 2.0 *Å* (6LDH) 16, of parvalbumin at 1.6 *Å* (5CPV) 2 and at 1.5 *Å* (4CPV) 3, of Trp-repressor domains at 2.2 *Å* (1WRP) 1 and at 1.8 *Å* (3WRP) 3. The residue Gln152 of sperm whale myoglobin is with positive $\phi$ in the structure at 1.4 *Å* (1MBD) and it is with negative $\phi$ in the structures at the 2.0 *Å* (1MBN, 2MBN) and 1.6 *Å* (1MBO).

*D: A relatively large amount of nonglycine residues with positive $\phi$ in the protein structure may be a simple indicator of local inaccuracies such as abnormally short distances between the nonbonded atoms, unusual valence bond lengths and bond angles and poor stereochemistry.* The inference is supported by the results of the analysis of the obsolete structure models 1RNS for ribonuclease S, 2GRS for glutathione reductase, 3FAB for immunoglobulin Fab-New, 4LDH for lactate dehydrogenase, all they at 2.0 *Å*. It is evident also from the analyses of the structure models with the PDB codes: 1ACX (2.00 *Å*) for actinoxanthin, 1HDS (1.98 *Å*) for deer sickle hemoglobin, 1NXB (1.38 *Å*) for neurotoxin B, 2SNS (1.54 *Å*) for staphylococcal nuclease, 2SOD (2.0 *Å*) for superoxide dismutase, and 6LDH (2.0 *Å*) for lactate dehydrogenase. The analyses of these structures have revealed the followings.

In 1ACX, there are several inadmissible short distances between the nonbonded atoms, for example, 0.61 *Å* between atoms *C* of Ser7 and $C^{\delta}$ of Pro8, 1.08 *Å* between atoms *O* of Ser7 and $C^{\delta}$ of Pro8, 1.30 *Å* between atoms *O* of Ala46 and *N* of Ala48, 1.43 *Å* between atoms *O* of Ala58 and Ala59, 1.87 *Å* between atoms *O* of Asp14 and Val64, 1.66 *Å* between atoms *O* of Ala92 and Asn98, 1.58*Å* between atoms *O* of Ala103 and *C* of Leu104, 1.59 *Å* between atoms $C^{\alpha}$ of Cys34 and Cys43, *etc.*. Unexpected is the conformation of Pro8 with the backbone angle $\phi$ = 107° and Phe106 bond angle *OCN* = 102°. In addition, the file 1ACX notes the incompleteness of the refinement of structure.

In 1HDS, there are 17 cis-peptide bonds and 32 peptide bonds deviating from the planarity by more than 50°. Residues Phe33 of subunit A, Val112 of subunit B and Asn116 of subunit D are in the unexpected D-isomeric form. There are too many conflicting short distances between the nonbonded atoms. A considerable number of the bond lengths and bond angles deviate from the expected standard values. Many of these bonds are either less than 1.0 *Å* or greater than 2.0 *Å* and bond angles are either less than 100° or greater than 130°. Torsion angle $\phi$ of the noticeable number of the equivalent nonglycine residues in the different subunits has different sign which testifies to the lack of similarity in the secondary structure of the subunits.

In 1NXB for neurotoxin B structure, there are unexpected values for several stereochemical parameters. Followings are the examples: for the *CN* bond 0.83 *Å* of Thr18 and 1.77 *Å* of Ser22, for the $NC^{\alpha}C$ bond angle 151° of Gly42 and 148° of Gly56, and for the $C^{\alpha}CN$ 149° of Lys47 and 141° of Glu58. This protein is probably identical to erabutoxin B from a Japanese sea snake as the 1NXB file remarks. The structural identity of the erabutoxin B and neurotoxin B and the existence of homology between all postsynaptic neurotoxins of the sea snake venom are noted also in the 3EBX file. There are several entries in the PDB on the structures of snake erabutoxins, e.g., 3EBX (1.4 *Å*), 5EBX (2.0

*Å*), 1QKD (1.49 *Å*), 1QKE (1.5 *Å*), 2ERA (1.81 *Å*), and 3ERA (1.7 *Å*). In these structure models, with positive $\phi$ are only 2 nonglycine residues, Ser8 and Val59, as distinct from 6 such residues in 1NXB (1.38 *Å*).

The staphylococcal nuclease structure 2SNS (1.54 *Å*) contains nonglycine residues with positive $\phi$ 17. The PDB file 2SNS remarks some inaccuracies in the structure. In particular, the electron density map does not distinctly reveal the location of residues 1 to 5, stereochemical parameters of some residues deviate from the expected values sufficiently. There are also unexpected closest contacts between the nonbonded atoms. The residues His46, Tyr115 and Gln123 are in the *D*-isomeric configuration in the A subunit. A number of entries are available in the PDB on staphylococcal nuclease structure deposited after 1992, e.g., with the PDB codes 1ENC, 2ENB, 1EYD, 1EZ8, 1KAA, 1SNM, 2SNM, 1STA, and 1STN. The number of nonglycine residues with positive $\phi$ in these structures is below 10. In particular, there are only six such residues in the 1.7 *Å* resolution structures 1EYD and 1STN.

In superoxide dismutase structure 2SOD (2.0 *Å*), a remarkable amount of inadmissible short distances are between the nonbonded atoms and a great deal of the bond lengths and bond angles deviate from the expected standard values. Many of the valence bonds are either less than 1.0 *Å* or greater than 2.0 *Å* and bond angles are either less than 100° or greater than 130°. In the four identical subunits of the protein, the torsion angle $\phi$ of some equivalent nonglycine residues has different sign. Of 40 nonglycine residues with positive $\phi$ present in the structure on the whole, only two residues (Leu124 and Asn137) are with positive $\phi$ in the all four identical subunits. For each of the remaining 32 residues with positive $\phi$, the equivalent residue is with negative $\phi$ in the some another subunit(s). It should be noted that there are with positive $\phi$ only 12 nonglycine residues in the 2.1 *Å* resolution structure of this protein 3SOD (Ser66, Leu124 and Asn137 in each of the four identical subunits). Only these residues are with positive $\phi$ also in the structure models 1E9P (1.7 *Å*) and 1Q0E (1.15 *Å*) of this protein deposited in the PDB after 1992.

Based upon above data, the following hypotheses may be speculated. The accuracy of structure models 1ACX for actinoxanthin and 1HDS for deer hemoglobin S is open to question; the new determination of the structure of these proteins is challenging. The structure models 1NXB for snake neurotoxin B, 2SNS for staphylococcal nuclease and 2SOD for superoxide dismutase are not accurate enough and should be attributed to obsolete ones.

**Table 1. Fractions of nonglycine residues with positive $\phi$ angle in the highest resolution 182 protein structures**

| 1 | 2 | 3 | 4 | 5 | 6 | 1 | 2 | 3 | 4 | 5 | 6 | 1 | 2 | 3 | 4 | 5 | 6 |
|---|---|---|---|---|---|---|---|---|---|---|---|---|---|---|---|---|---|
| 1A6M | 10 | 4 | 139 | 2 | 1.44 | 1TT8 | 11 | 13 | 151 | 3 | 1.99 | 2QXI | 20 | 14 | 202 | 7 | 3.47 |
| 1AEC* | 28 | 7 | 188 | 7 | 3.72 | 1UBQ* | 5 | 3 | 69 | 3 | 4.35 | 2R31 | 14 | 16 | 220 | 4 | 1.82 |
| 1AHO | 7 | 3 | 55 | 4 | 7.27 | 1UCS | 3 | 6 | 59 | 2 | 3.39 | 2RBK | 18 | 11 | 241 | 7 | 2.90 |
| 1ALC* | 5 | 2 | 115 | 6 | 5.22 | 1UFY | 5 | 8 | 114 | 2 | 1.75 | 2RH2 | 7 | 3 | 48 | 0 | 0.00 |
| 1BXO | 39 | 11 | 280 | 5 | 1.78 | 1UNQ | 5 | 6 | 111 | 3 | 2.70 | 2RHE* | 13 | 8 | 99 | 4 | 4.04 |
| 1BYI | 18 | 14 | 204 | 5 | 2.45 | 1UZV | 10 | 3 | 102 | 9 | 8.82 | 2SGA* | 32 | 4 | 147 | 4 | 2.72 |
| 1C7K | 14 | 8 | 116 | 1 | 0.86 | 1VBW | 6 | 4 | 60 | 1 | 1.67 | 2SN3* | 9 | 4 | 54 | 2 | 3.70 |
| 1CCR* | 11 | 9 | 98 | 1 | 1.02 | 1VL9 | 6 | 5 | 115 | 5 | 4.35 | 2V1M | 12 | 5 | 149 | 2 | 1.34 |
| 1CEX | 24 | 9 | 171 | 5 | 2.92 | 1X6Z | 13 | 6 | 114 | 1 | 0.88 | 2V8T | 28 | 18 | 272 | 4 | 1.47 |
| 1CSE* | 38 | 15 | 295 | 5 | 1.69 | 1X8Q | 10 | 3 | 172 | 4 | 2.33 | 2VB1 | 12 | 2 | 115 | 7 | 6.09 |
| 1DY5 | 2 | 4 | 118 | 1 | 0.85 | 1XMK | 3 | 2 | 74 | 0 | 0.00 | 2VHA | 17 | 12 | 258 | 8 | 3.10 |
| 1EB6 | 10 | 7 | 165 | 6 | 3.63 | 1Y55 | 10 | 3 | 108 | 0 | 0.00 | 2VHK | 24 | 12 | 180 | 8 | 4.44 |
| 1ECA* | 11 | 5 | 123 | 0 | 0.00 | 1YLJ | 22 | 13 | 239 | 8 | 3.35 | 2WFI | 18 | 7 | 152 | 8 | 5.26 |
| 1EXR | 11 | 2 | 133 | 0 | 0.00 | 1ZK4 | 28 | 8 | 221 | 5 | 2.26 | 2WUR | 20 | 10 | 203 | 6 | 2.96 |
| 1F94 | 3 | 0 | 58 | 2 | 3.45 | 1ZLB | 14 | 4 | 106 | 2 | 1.89 | 2XFR | 39 | 30 | 446 | 14 | 3.14 |
| 1FX1* | 18 | 2 | 127 | 5 | 3.94 | 1ZZK | 9 | 3 | 69 | 1 | 1.45 | 2XOD | 9 | 3 | 107 | 4 | 3.74 |
| 1G66 | 27 | 10 | 178 | 3 | 1.69 | 2A6Z | 19 | 9 | 201 | 11 | 5.47 | 2XU3 | 25 | 9 | 193 | 6 | 3.11 |
| 1G6X | 6 | 3 | 50 | 1 | 2.00 | 2APR* | 47 | 12 | 276 | 3 | 1.09 | 2Z6W | 21 | 7 | 141 | 4 | 2.84 |

| 1 | 2 | 3 | 4 | 5 | 6 | 1 | 2 | 3 | 4 | 5 | 6 | 1 | 2 | 3 | 4 | 5 | 6 |
|---|---|---|---|---|---|---|---|---|---|---|---|---|---|---|---|---|---|
| 1GCI | 35 | 13 | 232 | 4 | 1.72 | 2AYW | 25 | 8 | 199 | 6 | 3.02 | 2ZPM | 9 | 7 | 76 | 3 | 3.95 |
| 1GD1* | 23 | 11 | 309 | 6 | 1.94 | 2AZA* | 12 | 2 | 115 | 3 | 2.61 | 351C* | 7 | 6 | 73 | 1 | 1.37 |
| 1GP1* | 14 | 14 | 169 | 3 | 1.78 | 2BT9 | 11 | 2 | 77 | 1 | 1.30 | 3AKS | 27 | 7 | 162 | 6 | 3.70 |
| 1GQV | 2 | 12 | 131 | 1 | 0.76 | 2CCY* | 10 | 7 | 115 | 2 | 1.74 | 3BWH | 10 | 9 | 232 | 7 | 3.02 |
| 1GWE | 44 | 26 | 452 | 6 | 1.33 | 2CE2 | 11 | 3 | 153 | 5 | 3.27 | 3C2C* | 8 | 3 | 102 | 3 | 2.94 |
| 1HBG* | 19 | 3 | 126 | 1 | 0.79 | 2CGA* | 23 | 9 | 220 | 7 | 3.18 | 3CCD | 6 | 2 | 77 | 1 | 1.30 |
| 1HJ8 | 23 | 11 | 197 | 6 | 3.05 | 2CI2* | 2 | 4 | 61 | 2 | 3.28 | 3CYT* | 12 | 3 | 89 | 0 | 0.00 |
| 1IQZ | 6 | 5 | 73 | 5 | 6.85 | 2CPP* | 25 | 30 | 378 | 4 | 1.06 | 3D1P | 9 | 9 | 109 | 3 | 2.75 |
| 1IUA | 6 | 6 | 75 | 2 | 2.67 | 2CTS* | 33 | 22 | 402 | 5 | 1.24 | 3DFR* | 10 | 7 | 150 | 3 | 2.00 |
| 1IXB | 13 | 9 | 190 | 3 | 1.58 | 2CWS | 24 | 8 | 201 | 3 | 1.49 | 3DHA | 18 | 16 | 234 | 5 | 2.14 |
| 1J0P | 10 | 4 | 98 | 1 | 1.02 | 2DDX | 28 | 15 | 294 | 13 | 4.42 | 3DK9 | 41 | 19 | 419 | 12 | 2.86 |
| 1K4I | 16 | 13 | 198 | 3 | 1.52 | 2DSX | 5 | 5 | 45 | 0 | 0.00 | 3E4G | 10 | 5 | 164 | 6 | 3.66 |
| 1KWF | 36 | 11 | 325 | 8 | 2.46 | 2F01 | 16 | 1 | 103 | 2 | 1.94 | 3EA6 | 15 | 3 | 199 | 9 | 4.52 |
| 1L9L | 3 | 1 | 69 | 0 | 0.00 | 2FDN | 4 | 4 | 49 | 4 | 8.16 | 3EBX* | 5 | 4 | 55 | 2 | 3.64 |
| 1LH1* | 6 | 5 | 145 | 2 | 1.38 | 2FVY | 21 | 10 | 282 | 12 | 4.26 | 3F1L | 18 | 12 | 225 | 3 | 1.33 |
| 1LKK | 8 | 6 | 96 | 3 | 3.12 | 2FWH | 5 | 4 | 110 | 2 | 1.81 | 3F7L | 27 | 5 | 122 | 2 | 1.64 |
| 1LZ1* | 11 | 2 | 117 | 7 | 5.98 | 2G58 | 11 | 5 | 108 | 2 | 1.85 | 3FX5 | 13 | 5 | 84 | 2 | 2.38 |
| 1M1Q | 8 | 3 | 80 | 1 | 1.25 | 2GBA | 8 | 6 | 95 | 3 | 3.16 | 3HGP | 25 | 7 | 213 | 6 | 2.82 |
| 1M40 | 21 | 12 | 240 | 9 | 3.75 | 2GGC | 22 | 11 | 239 | 7 | 2.93 | 3G46 | 10 | 2 | 134 | 2 | 1.49 |
| 1MBA* | 11 | 6 | 133 | 0 | 0.00 | 2GKG | 11 | 5 | 109 | 2 | 1.83 | 3GOE | 1 | 2 | 77 | 4 | 5.19 |
| 1MJ5 | 24 | 21 | 272 | 9 | 3.31 | 2GUD | 22 | 3 | 97 | 2 | 2.06 | 3IP0 | 8 | 12 | 148 | 5 | 3.38 |
| 1MN8 | 5 | 10 | 88 | 3 | 3.41 | 2HMQ* | 6 | 3 | 106 | 2 | 1.89 | 3JYO | 31 | 9 | 249 | 0 | 0.00 |
| 1N55 | 16 | 10 | 231 | 3 | 1.30 | 2I4A | 8 | 6 | 97 | 4 | 4.12 | 3KFF | 8 | 0 | 142 | 5 | 3.52 |
| 1N9B | 20 | 11 | 244 | 11 | 4.51 | 2IIM | 6 | 3 | 54 | 1 | 1.85 | 3KLR | 9 | 4 | 114 | 3 | 2.63 |
| 1NKI | 12 | 5 | 120 | 0 | 0.00 | 2JFR | 25 | 12 | 207 | 1 | 0.48 | 3KS3 | 22 | 17 | 233 | 6 | 2.56 |
| 1NLS | 16 | 11 | 219 | 6 | 2.74 | 2JHF | 38 | 20 | 334 | 10 | 2.99 | 3M5Q | 29 | 30 | 326 | 5 | 1.53 |
| 1OD3 | 17 | 4 | 113 | 2 | 1.77 | 2LHB* | 6 | 5 | 141 | 1 | 0.71 | 3NIR | 4 | 5 | 40 | 0 | 0.00 |
| 1OK0 | 7 | 3 | 65 | 1 | 1.54 | 2LZM* | 11 | 3 | 152 | 2 | 1.32 | 3NOQ | 19 | 16 | 208 | 5 | 2.40 |
| 1OT9 | 13 | 4 | 110 | 1 | 0.91 | 2NRL | 13 | 5 | 130 | 1 | 0.77 | 3O4P | 32 | 20 | 280 | 12 | 4.29 |
| 1P1X | 16 | 8 | 232 | 4 | 1.72 | 2O9S | 6 | 4 | 59 | 0 | 0.00 | 3O5Q | 14 | 6 | 112 | 4 | 3.57 |
| 1PAZ* | 8 | 8 | 110 | 4 | 3.64 | 2OVO* | 4 | 3 | 50 | 2 | 4.00 | 3RP2* | 1 | 15 | 204 | 8 | 3.92 |
| 1PPT* | 1 | 4 | 33 | 1 | 3.03 | 2P5K | 3 | 1 | 58 | 1 | 1.72 | 3WRP* | 5 | 3 | 94 | 3 | 3.19 |
| 1PQ7 | 34 | 9 | 188 | 5 | 2.66 | 2PAB* | 7 | 6 | 105 | 3 | 2.86 | 4DFR* | 10 | 10 | 147 | 3 | 2.04 |
| 1R2M | 5 | 5 | 63 | 3 | 4.76 | 2PKA* | 22 | 15 | 206 | 7 | 3.40 | 4GCR* | 13 | 8 | 159 | 9 | 5.66 |
| 1R6J | 7 | 2 | 73 | 4 | 5.48 | 2PND | 8 | 5 | 109 | 3 | 2.75 | 5CPA* | 23 | 10 | 282 | 5 | 1.77 |
| 1REI* | 8 | 6 | 97 | 3 | 3.09 | 2PNE | 37 | 5 | 42 | 0 | 0.00 | 5ER2* | 38 | 13 | 290 | 2 | 0.69 |
| 1RNT* | 12 | 4 | 90 | 3 | 3.33 | 2PPP | 12 | 7 | 93 | 2 | 2.15 | 5TNC* | 13 | 1 | 146 | 2 | 1.37 |
| 1RTQ | 19 | 12 | 270 | 7 | 2.59 | 2PVB | 7 | 1 | 98 | 2 | 2.04 | 6LDH* | 24 | 10 | 303 | 16 | 5.28 |
| 1SSX | 31 | 4 | 165 | 4 | 2.42 | 2PVE | 5 | 6 | 45 | 0 | 0.00 | 6PCY* | 11 | 5 | 87 | 0 | 0.00 |
| 1TG0 | 3 | 4 | 61 | 1 | 1.64 | 2PWA | 33 | 9 | 244 | 8 | 3.28 | 8FAB* | 35 | 28 | 389 | 15 | 3.86 |
| 1THB* | 20 | 14 | 263 | 2 | 0.76 | 2PYA | 5 | 5 | 45 | 0 | 0.00 | 9PAP* | 28 | 10 | 182 | 3 | 1.65 |
| 1TON* | 20 | 13 | 203 | 6 | 2.96 | 2QCP | 4 | 4 | 74 | 2 | 2.70 | 9WGA* | 40 | 6 | 128 | 11 | 8.59 |
| 1TQG | 5 | 1 | 98 | 1 | 1.02 | 2QSK | 14 | 9 | 79 | 2 | 2.53 | | | | | | |

*The columns present: 1, the PDB code of structure; 2 to 5, the number of the glycine, proline, nonglycine, and with positive $\phi$ nonglycine residues; 6, the percentage fraction of nonglycine residues with positive $\phi$ in the structure. "*" indicates the PDB codes of 52 'old', deposited in the PDB by 1992 structures. The data given are on the: first subunit of the two identical subunits of 1DY5, 1GP1, 1IXB, 1LNI, 1M1Q, 1NKI, 1OT9, 1R2M, 1REI, 1THB, 1Y55, 2CCY, 2CGA, 2F01, 2GUD, 2HS1, 2JHF, 2V8T, 2VHA, 2Z6W, 3CCD, 3CYT, 3F1L, 3FX5, 3G46, 3RP2, 4DFR, and 9WGA; three identical subunits of 2BT9 and 2PVE; four identical subunits of 1GD1, 1UZV and 2HMQ; second subunit of the two identical subunits of 2AZA, 2PAB and 3NOQ; fourth subunit of the four identical subunits of 1MN8 and 2JHF; third and fourth subunits of the two pairs identical subunits of 2PKA and 8FAB. Gly278 and Asp279 in 1BXO, Leu64 and Val68 in 2WUR and Asn67 and Gly68 in 1DY5 were omitted from the consideration (with account of the remarks of corresponding files)*

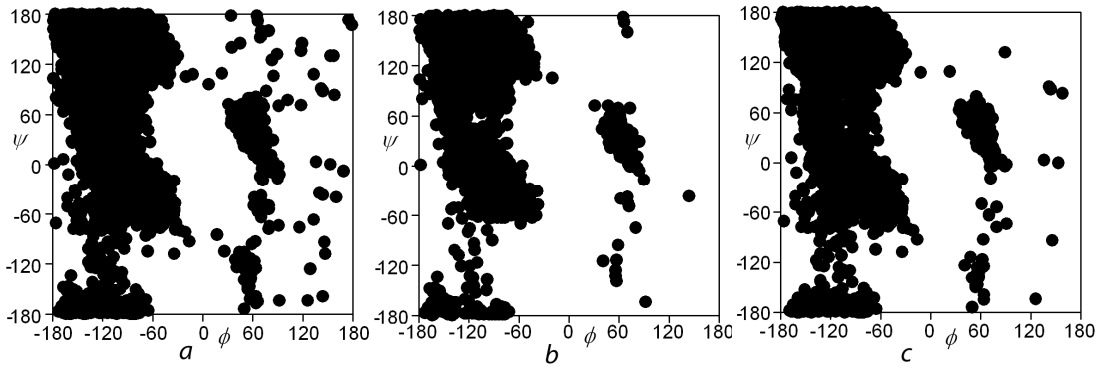


**Fig. 1. Ramachandran plots of ($\phi,\psi$) angles for nonglycine residues in the 182 highest resolution largely nonhomologous protein structures**

*(a) Total nonglycine residues. (b) Total His, Asp and Asn residues. (c) Total nonglycine residues with exception of His, Asp and Asn residues*



*Peer-review history:*
*The peer review history for this paper can be accessed here:*
*http://sciencedomain.org/review-history/20990*